Published in final edited form as:
Thromb Res. 2012 September ; 130(3): e163–e170. doi:10.1016/j.thromres.2012.05.021.

Inhibition of tissue factor by ixolaris reduces primary tumor growth and experimental metastasis in a murine model of melanoma

Andreia Da Silva de Oliveira[1,a], **Luize G Lima**[1,a], **Andréa Mariano-Oliveira**[1], **Daniel E Machado**[2], **Luiz E Nasciutti**[2], **John F Andersen**[3], **Lars C Petersen**[4], **Ivo M B Francischetti**[3], and **Robson Q Monteiro**[1,b]

[1]Instituto de Bioquímica Médica, Universidade Federal do Rio de Janeiro, Rio de Janeiro, Brazil

[2]Instituto de Ciências Biomédicas, Universidade Federal do Rio de Janeiro, Rio de Janeiro, Brazil

[3]Vector Biology Section, National Institutes of Health, Bethesda, MD, USA

[4]Biopharmaceutical Research Unit, Novo Nordisk, Maalov, Denmark

Abstract

Melanoma is a highly metastatic cancer and there is strong evidence that the clotting initiator protein, tissue factor (TF), contributes to its aggressive pattern. TF inhibitors may attenuate primary tumor growth and metastasis. In this study, we evaluated the effect of ixolaris, a TF inhibitor, on a murine model of melanoma B16F10 cells. Enzymatic assays performed with B16F10 and human U87-MG tumor cells as the TF source showed that ixolaris inhibits the generation of FX in either murine, human or hybrid FVIIa/TF complexes. The effect of ixolaris on the metastatic potential was further estimated by intravenous injection of B16F10 cells in C57/BL6 mice. Ixolaris (250 μg/kg) dramatically decreased the number of pulmonary tumor nodules (4 ± 1 compared to 47 ± 10 in the control group). Furthermore, a significant decrease in tumor weights was observed in primary tumor growth assays in animals treated with ixolaris (250 μg/kg) from days 3 to 18 after a subcutaneous inoculation of melanoma cells. Remarkably, immunohistochemical analyses showed that inhibition of melanoma growth by ixolaris is accompanied by a significant downregulation of both vascular endothelial growth factor (VEGF) expression and microvascular density in the tumor mass. Our data demonstrate that ixolaris targets B16F10 cell-derived TF, resulting in the reduction of both the primary tumor growth and the metastatic potential of melanoma, as well as the inhibition of tumor angiogenesis. Therefore TF may be a potential target for the treatment of this aggressive malignancy.

Keywords

Tissue factor; melanoma; ixolaris; angiogenesis; metastasis; anticoagulant therapy

[b]Corresponding author. Instituto de Bioquímica Médica/CCS/UFRJ, Avenida Carlos Chagas Filho 373, Cidade Universitária, Ilha do Fundão, Rio de Janeiro, 21941-590, Brazil. Tel: +55 212562 6782; fax: +55 212270 8647. robsonqm@bioqmed.ufrj.br (R.Q. Monteiro) .
[a]These authors contributed equally to this work.

Conflict of interest statement
The authors declare that they have no competing interests.

Authors' contributions
ASO and LGL participated in the design of the study, performed the acquisition and the analysis of the data and drafted the manuscript; AMO, DEM and LEN performed research and contributed to the analysis of the data; JFA, LCP and IMBF provided vital reagents and resources and helped draft the manuscript; RQM conceived the study, participated in its design and coordination, and helped draft the manuscript. All authors read and approved the final manuscript.

In 1865, Armand Trousseau first described an important relationship between cancer and thrombosis. Blood disorders involving the hyperactivation of the coagulation system and formation of intravascular fibrin clots (thrombosis) may be the first sign of a malignant tumor [1,2]. This correlation is exemplified by the abnormally elevated expression of the clotting initiator protein, tissue factor (TF), on the surface of tumor cells. The presence of elevated TF levels in plasma, mainly incorporated into tumor-derived microvesicles, would allow the formation of the TF/factor VIIa (FVIIa) complex and the subsequent activation of blood coagulation reactions. This condition has been correlated with both disseminated intravascular coagulation and thrombosis occurrence [3,4].

TF is expressed in many types of cancers [5-7] and studies employing cultured cells as well as patient specimens have demonstrated a strong correlation between TF expression and aggressive tumor behavior [8-10]. In particular, TF procoagulant activity has been correlated with the metastatic potential of tumor cells [11,12]. In addition, TF expression correlates with increased tumor angiogenesis, as reported in studies on patient samples from non-small cell lung, colorectal, hepatocellular, and pancreatic cancer [13-16]. It is therefore proposed that TF expression leads to an unbalanced production of anti- and/or proangiogenic factors such as vascular endothelial growth factor (VEGF), which favors increased tumor vasculature [6,17]. Along with its role in initiating blood coagulation reactions, the TF/FVIIa complex may modulate intracellular signaling through cleavage of the G protein-coupled protease-activated receptor-2 (PAR2). *In vitro* and *in vivo* assays have demonstrated that PAR2 activation is correlated with the production of tumor-promoting molecules, primary tumor growth and the proangiogenic and invasive properties of tumors [18]. Remarkably, some of these effects seem to be independent of the procoagulant activity of the TF/FVIIa complex [19].

Melanoma, the most common fatal form of skin cancer, is an aggressive, therapy-resistant malignancy of melanocytes that represents a significant public health burden because its incidence is increasing in Caucasian populations across the world [20]. The prognosis of patients diagnosed with metastatic melanoma is very poor, with a limited number of agents available for treatment [21]. Several lines of evidence indicate a key role for blood clotting activation in melanoma progression, suggesting that TF is a target for adjuvant treatment of this aggressive cancer [22-24].

Ixolaris, a tick salivary 140 amino acid protein containing 10 cysteines and 2 Kunitz-like domains, binds to FXa or FX as scaffolds for the inhibition of the TF/FVIIa complex, in which the FVIIa catalytic site is inactivated, as previously demonstrated by inhibition of macromolecular (i.e., FX and FIX) substrates [25]. Ixolaris does not bind to the active site cleft of FXa. Instead, complex formation is mediated by the FXa heparin-binding exosite [26]. In addition, ixolaris interacts with zymogen FX through a precursor state of the heparin-binding exosite [27]. Because ixolaris displays potent and long-lasting antithrombotic activity [28], we hypothesized that this molecule might interfere with melanoma progression. Here, we demonstrate that ixolaris inhibits human and murine TF procoagulant activity to a similar extent. Consequently, ixolaris decreases both primary tumor growth and experimental metastasis in a murine melanoma model. Inhibition of tumor growth was accompanied by the downregulation of VEGF expression and a decrease in vessel density in tumor mass. Therefore, ixolaris displays potential antitumor effects, emerging as a valuable tool for studying the role of TF in melanoma biology.

MATERIALS AND METHODS

Reagents

Recombinant ixolaris was produced in High Five insect cells (Invitrogen, San Diego, CA), as previously described by Francischetti et al. [25], and purified and quantified as described [28]. Recombinant nitrophorin-2 was produced in *Escherichia coli*, purified, and quantified as previously described [29]. Both human FX and murine FX were purchased from Haematological Technologies Inc. (Essex Junction, VT, USA). Human FVIIa was purchased from American Diagnostica (Greenwich, CT, USA). Murine FVIIa was expressed and purified as previously described [30]. The chromogenic substrate for FXa (S-2765, N-α-benzyloxycarbonyl-D-Arg-Gly-Arg-p-nitroanilide) was purchased from Diapharma (Westchester, OH). The PAR1 agonist peptide (PAR1-AP, TFLLR-NH2) and the PAR2 agonist peptide (PAR2-AP, SLIGKL-NH2) were synthesized by Biosynthesis Inc. (Lewisville, TX, USA).

Cell culture

The murine melanoma cell line B16F10 was grown at 37°C in a humidified, 5% CO_2 atmosphere, in Dulbeccós modified Eagle medium (DMEM; GibcoBRL) at pH 7.2, containing 10% (v/v) foetal bovine serum (FBS) and supplemented with 2.4 g/L HEPES, 3.7 g/L sodium bicarbonate, 125 mg/L sodium dihydrogen phosphate, 110 mg/L sodium pyruvate, 100,000 U/L penicillin, 100 mg/L streptomycin and 2 mM L-glutamine. Cells were detached with Hank's solution containing 10 mM HEPES and 0.2 mM EDTA, spun at 350 × g for 7 min, resuspended in DMEM (supplemented as described above) and transferred to another culture flask. The human glioblastoma cell line, U87-MG, was grown at 37°C in a humidified, 5% CO_2 atmosphere, in DMEM-F12 (GibcoBRL) containing 10% (v/v) FBS and supplemented with 2 g/L HEPES, 60 mg/L penicillin, 100 mg/L streptomycin and 1.2 g/L sodium bicarbonate. Cells were washed twice with phosphate buffered saline (PBS), detached with Hank's solution containing 10 mM HEPES and 0.2 mM EDTA, spun at 350 × g for 7 min, resuspended in DMEM-F12 (supplemented as described above) and transferred to another culture flask.

FX activation as measured by hydrolysis of a chromogenic substrate

Activation of FX by FVIIa was performed as previously described [31] in 50 mM HEPES, 100 mM NaCl, 5 mM $CaCl_2$, and 1 mg/mL BSA, pH 7.5 (HEPES-BSA buffer). Murine FVIIa (1 nM) was incubated with U87-MG or B16F10 cells (5×10^4/mL) for 10 min at 37°C. The reaction was initiated by the addition of murine FX (135 nM), and 25 μL aliquots were transferred after 30 min into microplate wells containing 25 μL of Tris-EDTA buffer (50 mM Tris-HCl, 150 mM NaCl, 20 mM EDTA, and 1 mg/mL polyethyleneglycol 6000, pH 7.5). Alternatively, human FVIIa (1 nM) was incubated with U87-MG cells (5×10^4/mL) for 10 min at 37°C prior to the addition of human FX (135 nM). After the addition of 50 μL of 200 μM S-2765, prepared in Tris-EDTA buffer, the absorbance at 405 nm was recorded at 37°C for 30 min using a Spectramax Microplate Reader (Molecular Devices, Menlo Park, CA, USA). The velocities (mOD/min) obtained in the first minutes of the reaction were used to calculate the amount of formed FXa, as compared to a standard curve using known enzyme concentrations. The appropriate controls performed in the absence of cells or in the absence of FVIIa showed no significant FXa formation.

The inhibitory effect of ixolaris was evaluated by incubating FX with varying amounts of the inhibitor (0-5 nM) for 10 min prior to adding it to the FVIIa and tumor cells. FXa formed in the absence of ixolaris was taken as 100%.

Quantification of experimental melanoma metastasis

Eight week-old C57BL/6 mice maintained at our own facilities were injected via the lateral tail vein with a 100 μL-bolus of 2.5×10^5 B16F10 cells (resuspended in DMEM). The anti-metastatic effect of ixolaris or nitrophorin-2 was evaluated by the intravenous injection of 250 μg/kg ixolaris or nitrophorin-2 two hours before the inoculation of B16F10 cells. The control animals were injected with PBS instead of the coagulation inhibitor. After 15 days, the animals were sacrificed, the lungs were removed, and the number of pulmonary tumor nodules only on the convex face of the organ was counted. The animal experiments were performed under approved protocols of the institutional animal use and care committee (Institute of Medical Biochemistry, Federal University of Rio de Janeiro).

Primary tumor growth assay

B16F10 cells (3.5×10^5, resuspended in DMEM) were subcutaneously inoculated into the flank of 8-week-old C57BL/6 mice. Treatment with 50 or 250 μg/kg ixolaris, or 250 μg/kg nitrophorin-2 (diluted in PBS, 100 μL of final volume intraperitonealy inoculated) was initiated 3 days after the tumor cell inoculation and continued daily for 15 days. The control animals were injected with PBS instead of the coagulation inhibitor. Tumor weights were determined at the time of sacrifice. The animal experiments were performed under approved protocols of the institutional animal use and care committee (Institute of Medical Biochemistry, Federal University of Rio de Janeiro).

Immunohistochemistry

Primary tumors were removed from mice at the time of sacrifice (day 18 after tumor cell inoculation) and fixed in 4% formaldehyde. Tissue staining was performed on paraffin-embedded sections (4 μm-thick), which were incubated overnight, following heat antigen retrieval, with either a monoclonal antibody, anti-mouse endoglin (CD105) (MAB-1320, R&D Systems, USA) at 1:10 dilution, or a monoclonal antibody against VEGF (SC-7269, Santa Cruz Biotechnology, Santa Cruz, CA) at 1:100 dilution. In order to reduce nonspecific antibody binding, the sections were incubated with PBS containing 10% nonimmune goat serum, 5% BSA and 10% FBS for 30 min prior to incubation with the primary antibodies. The sections were further processed using a LSAB2-HRP Kit (Dako-Cytomation, Carpinteria, CA), with diaminobenzidine (3, 3′-diaminobenzidine tablets; Sigma Chemical Co, St. Louis, MO, USA) as the chromogen and hematoxylin as the counterstain. The negative control slides consisted of sections incubated with antibody vehicle or nonimmune rat or mouse serum. Ten fields of each immunostained section (CD105 and VEGF) from each specimen were chosen at random and captured. These high-quality images (2048 × 1536 pixels buffer) were quantified using Image Pro Plus 4.5.1 (Media Cybernetics, Silver spring, MD). Data were stored in Adobe Photoshop 3.0, for illumination and background color corrections. The number of transversal sections of CD105 was counted, and these numbers per square millimeter of the tumor were calculated, as previously described [32]. A semiquantitative evaluation of immunohistochemical staining for VEGF was performed as previously described [32].

RNA isolation and reverse transcriptase polymerase chain reaction

RNA was isolated from B16F10 cells (5×10^5) using the Trizol reagent (Invitrogen) following the manufacturer's instructions. Total RNA (1 μg) was reverse-transcribed into cDNA using the High-Capacity cDNA Reverse-Transcription Kit by Applied Biosystems following the manufacturer's protocol. All samples were previously treated with RNase-free DNase I (Fermentas).

Real-time polymerase chain reaction

Primer pairs for PAR1, PAR2 and β-actin were designed using the OLIGO Primer Analysis Software. The primer pair sequences are listed in Table 1. Each PCR reaction sample consisted of 7.5 μL of QuantiFast SYBR Green PCR Kit (Qiagen), 5.75 μL dH_2O, 0.37 μL of each of the forward and reverse primers (0.25 nmol), and 1 μL of single-strand complementary DNA (cDNA) in a final reaction volume of 15 μL.

Gene expression was detected by the QuantiFast SYBR Green PCR Kit (Qiagen) on a Rotor-gene 6000 Real-Time PCR system (Corbett, NSW, Australia). The expression of each gene was calculated relative to the β-actin in each sample. The PCR cycling program was 95°C for 30 s and 60°C for 45 s, and then repeated 40 times. Each reaction was carried out in duplicate. The relative expression level of each target gene was calculated by the relative standard curve and ΔΔCt methods using Rotor-gene 6000 software (Rotor-gene 6000 series software 1.7, Info-ZIP Pty Ltd, Australia). The quantification was normalized to an endogenous control (the housekeeping gene β-actin), and standard curves were prepared for each target and the endogenous reference (β-actin) genes.

Analysis of ERK 1/2 phosphorylation by Western blot

B16F10 cells were seeded in 6-well plates at a concentration of 5 ± 10^5 cells/well. The levels of phospho-ERK 1/2, downstream products of the MAPK/ERK pathway, which are known to be induced by PAR activation, were examined. Briefly, cells were serum-starved for 30 min before treatment with 50 μM agonist peptides for PAR1 (PAR1-AP, TFLLR-NH2) or PAR2 (PAR2-AP, SLIGKL-NH2) for 0, 5, 10, 15, 30, and 60 min. Cell lysates were separated by SDS-polyacrylamide gel electrophoresis (SDS-PAGE, 10%). Proteins were transferred onto polyvinylidene fluoride (PVDF) membranes (Amersham Pharmacia Biotech) and further blocked with Tris-buffered saline (TBS) containing 5% BSA and 0.1% Tween 20 for 1 h at room temperature. The membranes were then probed with primary antibodies overnight at 4°C. The membranes were washed three times with TBS/Tween before adding secondary antibodies for 1 h at room temperature. The membranes were further washed and probed with peroxidase-conjugated streptavidin for 1h at room temperature. Immunodetection was carried out by a chemiluminescent method using the Western Lightning ECL kit (Amersham Pharmacia Biotech). The blots were quantified using the Scion Image software. The relative levels of phospho-ERK 1/2 were expressed as the ratio to total ERK 1/2.

Quantification of VEGF by immunoassay

Cells were serum-starved for 30 min prior to stimulation with PAR1 (PAR1-AP, TFLLR-NH2, 50 μM) or PAR2 (PAR2-AP, SLIGKL-NH2, 50 μM) agonist peptides for 24 h at 37°C. The VEGF protein secretion into the cell supernatants was measured using a human VEGF ELISA kit from Pepro Tech Inc. (Rocky Hill, NJ) following the manufacturer's instructions.

Statistical analysis

One-way ANOVA tests or unpaired *t* tests were performed using the InStat software (GraphPad, USA).

RESULTS

Ixolaris blocks both murine and human TF procoagulant activities

Ixolaris effectively inhibits the TF/FVIIa complex-mediated activation of FX in assays employing purified human coagulation factors [25]. Given that our *in vivo* experiments were

carried out in mice, it was necessary to examine whether ixolaris displays inhibitory activity toward the murine extrinsic tenase complex using murine coagulation factors. This experiment was also important given that human and murine TF display important structural differences, which indicates poor species compatibility between murine TF and human FVIIa [30,33]. We investigated the ability of ixolaris to inhibit autologous TF/FVIIa complexes of murine and human origins. Figure 1 shows that ixolaris blocked FX activation by both complexes (U87-MG glioblastoma and B16F10 melanoma cells employed as human and murine TF sources, respectively) to a similar extent. Ixolaris also inhibited a heterologous complex between human tumor cell-derived TF and murine FVIIa, which mimics the condition observed in murine xenograft models employing human cell lines (Figure 1).

Ixolaris impairs the establishment of B16F10 melanoma cells *in vivo*

Previous studies showed that TF expression plays an essential role in experimental melanoma metastasis [11,23]. Therefore, we evaluated the effects of ixolaris on the metastastic capacity of B16F10 cells. Using a murine model, we observed that a single dose of ixolaris (250 μg/kg) given 2 h berfore the intravenous inoculation of melanoma cells in C57BL/6 mice dramatically decreased the number of pulmonary tumor nodules (4 ± 1, n=15) as compared to the control group (47 ± 10, n=8) (Figure 2A).

TF expression has also been correlated with primary tumor growth, which has led different authors to propose TF inhibition as a potential antitumor therapeutic strategy [34,35]. Therefore, we examined the ability of ixolaris to reduce the primary tumor growth initiated by subcutaneous inoculation of B16F10 cells in C57BL/6 mice. Daily treatment with ixolaris, initiated 3 days after cells inoculation, produced a significant reduction in the tumor weights in animals treated with 250 μg/kg of ixolaris (0.6 ± 0.6 g) as compared to the control group (1.8 ± 0.8 g) (Figure 2B). No significant effect has been observed in animals treated with 50 μg/kg of ixolaris (1.3 ± 0.8 g). *In vitro* assays for cell proliferation and viability showed no direct toxic effect of ixolaris on tumor cells (data not shown).

The antitumor effect of coagulation inhibitors targeting TF has been associated with diminished angiogenesis [19,35]. Therefore, we further employed immunohistochemistry analysis to determine whether impairment of subcutaneous melanoma growth by ixolaris was accompanied by a reduction in VEGF expression and in the vessel density in primary tumors. Daily treatment with ixolaris significantly diminished VEGF expression (Figure 3A) and the vessel density in tumors (Figure 3B), as assessed by CD105 staining. Taken together, these results indicate a potent antitumor effect of ixolaris, in addition to an important association between tumor angiogenesis reduction and this effect.

Nitrophorin-2, a FIX/FIXa inhibitor, decreases metastasis but has no effect on the primary growth of melanoma cells

Inhibition of the TF/FVIIa complex by ixolaris results in decreased thrombin formation by downstream coagulation reactions. In order to discriminate whether the antitumor effect of ixolaris was due to a blockade of the TF/FVIIa complex or the downstream generation of coagulation enzymes, we tested nitrophorin-2, a FIX/FIXa inhibitor which potently inhibits coagulation *in vitro* and *in vivo* mainly through blockade of the intrinsic tenase complex assembly [36,37]. Similar to ixolaris, nitrophorin-2 treatment significantly decreased the number of pulmonary melanoma metastases in C57BL/6 mice (3 ± 1, n=7) as compared to the control group (15 ± 4, n=8) (Figure 4A). Conversely, no effect on the primary tumor growth of B16F10 cells was observed in nitrophorin-2-treated animals, as assessed by measurement of the tumor weights (1.5 ± 1.4 g vs. 1.6 ± 0.8 g in the control group) (Figure 4B).

Activation of PAR2 in B16F10 cells stimulates VEGF production

We have previously demonstrated that B16F10 cells express elevated levels of TF as compared to the murine melanocyte cell line melan-a [38]. Most of the pro-tumor effects of TF and blood clotting enzymes have been attributed to cellular signaling induced by the protease-activated receptors PAR1 and PAR2. To gain insight into the mechanisms underlying TF participation in melanoma progression, we evaluated the activation of PAR1 and PAR2 in B16F10 cells. Real-time PCR analysis demonstrated that B16F10 cells constitutively express PAR1 and PAR2 at similar levels (Figure 5A). The incubation of B16F10 cells with synthetic PAR1 and PAR2 agonist peptides induced ERK 1/2 phosphorylation in a time-dependent fashion, indicating the functional expression of both receptors (Figure 5B). However, PAR2, but not PAR1, activation increased the production of the pro-angiogenic factor VEGF by B16F10 cells, as shown in Figure 5C (see Discussion).

DISCUSSION

Several lines of evidence indicate that activation of blood coagulation facilitates tumor progression, in which distinct events are linked to metastasis and/or primary tumor growth. The correlation between the procoagulant properties of tumor cells and metastatic potential has been well established. TF procoagulant activity, which is mediated by its extracellular domain, is crucial for the establishment of tumor cells at distant sites, as demonstrated in melanoma, breast cancer and fibrosarcoma models [11,12,19]. The role of coagulation activation in tumor cell dissemination is further supported by the ability of a number of anticoagulants, including the thrombin inhibitor hirudin [39], FXa inhibitors, such as NAP5 (Nematode Anticoagulant Protein 5) [40], and ACAP (Ancylostoma caninum Anticoagulant Peptide) [41], to decrease experimental metastasis. In addition, genetically altered mice defective in different coagulation proteins, such as prothrombin [12,42], factor VIII [43], fibrinogen [42] and FXIII [44], have a decreased susceptibility to experimental metastasis. Altogether, it is clear that coagulation activation by tumor cells plays an essential role in tumor cell dissemination.

In this report, we demonstrated that ixolaris blocks both human and murine TF procoagulant activity *in vitro*. These findings are particularly relevant because they validate the use of ixolaris as a tool to study the role of TF-dependent processes in murine models of cancer. Accordingly, ixolaris effectively blocks the experimental metastasis of B1610 cells *in vivo* at relatively low concentrations (microgram/kg). Because ixolaris effectively inhibits TF activity, it is conceivable that the inhibition of coagulation activation, platelet aggregation and fibrin formation prevents the successful implantation of tumor cells for the generation of lung metastases. This process has been linked to the activation of the PAR1 by thrombin on tumor cells, including B16F10 melanoma, which facilitates tumor metastasis [45]. Notably, Bromberg and colleagues [46] showed that overexpression of PAR1 in low TF-expressing tumor cells is not sufficient to increase their metastatic potential. However, acquisition of the pro-metastatic role of PAR1 *in vivo* is observed upon co-expression of PAR1 and TF on tumor cells. Considering that B16F10 cells display an appropriate membrane surface for the assembly of thrombin-generating complexes [38,47], the blockade of the TF/FVIIa complex by ixolaris may prevent PAR1 activation and contribute to its antimetastatic activity. However, further studies employing ixolaris in spontaneous models of melanoma metastasis will clarify whether this protein interferes with the first steps of tumor dissemination.

A role for PAR1 in primary tumor growth has also been proposed [48]. Strategies targeting PAR1 have been successfully used to counteract the *in vivo* primary growth of melanoma [49] and breast cancer cell lines [50]. Here, we demonstrated that ixolaris significantly reduces B16F10 primary growth in the microgram/kg range. This effect may result, at least

in part, from the blockade of TF-mediated procoagulant properties, accounting for reduced thrombin generation and down regulation of PAR1 activation in the tumor microenvironment. This hypothesis is supported by primary tumor growth assays employing hirudin, which reduces tumor progression in the B16F10 model [51].

In contrast to PAR1 inhibition, blocking PAR2 signaling in tumor cells has a minor impact on tumor metastasis. A non-anticoagulant monoclonal antibody that blocks TF-mediated signaling through PAR2 [11,19] or deletion of the TF cytoplasmic domain [12] have no impact on tumor metastasis. These data strongly suggest that, in opposition to TF-mediated coagulation, TF-mediated signaling is not critical for the metastatic potential of tumor cells. In contrast, blocking of TF-mediated signaling through PAR2 with anti-TF or anti-PAR2 antibodies decreases primary tumor growth and reduces tumor angiogenesis in a human breast cancer model. These observations are supported by studies employing a spontaneous murine breast cancer model in which the PAR2, but not PAR1, genetic deficiency delays tumor growth and angiogenesis [52]. Herein, we demonstrate that the inhibitory effect of ixolaris on B16F10 primary growth is accompanied by decreased VEGF expression in the tumors as well as reduced angiogenesis. These observations are consistent with our previous work employing a human glioblastoma model in nude mice in which ixolaris decreased U87-MG primary growth and tumor vessel formation *in vivo* [35]. Because PAR2, but not PAR1, mediated VEGF production by B16F10 cells *in vitro* (Figure 5C), we speculate that blockade of TF/FVIIa/PAR2-coupled signaling by ixolaris may contribute to its antitumor and antiangiogenic effects. In accordance with this hypothesis, we recently observed that TF/FVIIa/PAR2-coupled signaling mediates VEGF production by U87-MG cells *in vitro* [53].

Consistent with the role of blood clotting proteins in tumor metastasis, Langer et al. [43] reported that mice displaying hemophilia A are significantly protected against the metastatic potential of B16F10 cells. Contrarily, the primary tumor growth is unaltered in hemophilic mice. These data are in accordance with our observations that nitrophorin-2, a potent FIX/FIXa inhibitor, decreases metastasis but has no effect on primary tumor growth (Figure 4). Together, these results suggest that thrombin generation in the B16F10 tumor microenvironment is not dependent on components of the intrinsic coagulation pathway, such as FIX and FVIII. However, the effect of ixolaris on primary B16F10 tumor growth suggests that the activation of FX into FXa by TF/FVIIa is critical for thrombin generation in the tumor microenvironment. Therefore, both nitrophorin-2 and ixolaris emerge as important tools for studying the role of blood clotting proteins in tumor biology.

In conclusion, ixolaris is a potent anticoagulant that blocks the procoagulant properties of both human and murine TF, regardless of the species-specific differences in this cofactor. Notably, despite its long half-life (> 24 h, [28]), ixolaris treatment does not result in major bleeding when repeatedly administered in animal models [35]. In addition, ixolaris displays antimetastatic, antitumor and antiangiogenic effects in the microgram/kg range, possibly through the combined action against the procoagulant and the pro-signaling properties of TF. It is reasonable to speculate that TF overexpressed in tumor tissues of patients with melanoma [54], as well as in other tumor types, could direct ixolaris to tumor microenvironment, as Cocco and colleagues have shown for the TF-antagonist hI-con1™ (Iconic Therapeutics, Inc., Atlanta, GA) [55]. In this context, ixolaris might be regarded as a potential antitumor drug against TF-expressing tumors.

Acknowledgments

We would like to thank Jorgeane Freire e Souza for her technical assistance. This research was supported by Conselho Nacional de Desenvolvimento Científico e Tecnológico (CNPq), Fundação de Amparo à Pesquisa do Estado do Rio de Janeiro Carlos Chagas Filho (FAPERJ), Fundação do Câncer and Coordenação de

Aperfeiçoamento de Pessoal de Nível Superior (CAPES). This work was supported in part by the Intramural Research Program of the Division of Intramural Research, National Institute of Allergy and Infectious Diseases, National Institutes of Health (NIH). Because JFA and IMBF are government employees and this is a government project, the work is in the public domain in the United States. Notwithstanding any other agreements, the NIH reserves the right to provide the work to PubMedCentral for display and use by the public, and PubMedCentral may tag or modify the work consistent with its customary practices. You can establish rights outside of the U.S. subject to a government use license.

Abbreviations

TF	tissue factor
VEGF	vascular endothelial growth factor
PAR1/2	protease activated receptor-1/2
ERK	extracellular-signal regulated kinase

References

[1]. Rickles FR, Falanga A. Molecular basis for the relationship between thrombosis and cancer. Thromb Res. 2001; 102:V215–V224. [PubMed: 11516455]

[2]. Sud R, Khorana AA. Cancer-associated thrombosis: risk factors, candidate biomarkers and a risk model. Thromb Res. 2009; 123(Suppl 4):S18–S21. [PubMed: 19303497]

[3]. Davila M, Amirkhosravi A, Coll E, Desai H, Robles L, Colon J, et al. Tissue factor-bearing microparticles derived from tumor cells: impact on coagulation activation. J Thromb Haemost. 2008; 6:1517–24. [PubMed: 18433463]

[4]. Lima LG, Oliveira AS, Campos LC, Bonamino M, Chammas R, Werneck C, et al. Malignant transformation in melanocytes is associated with increased production of procoagulant microvesicles. Thromb Haemost. 2011; 106:712–23. [PubMed: 21800005]

[5]. Kakkar AK, Lemoine NR, Scully MF, Tebbutt S, Williamson RC. Tissue factor expression correlates with histological grade in human pancreatic cancer. Br J Surg. 1995; 82:1101–4. [PubMed: 7648165]

[6]. Rak J, Milsom C, May L, Klement P, Yu J. Tissue factor in cancer and angiogenesis: the molecular link between genetic tumor progression, tumor neovascularization, and cancer coagulopathy. Semin Thromb Hemost. 2006; 32:54–70. [PubMed: 16479463]

[7]. Ribeiro FS, Simao TA, Amoedo ND, Andreollo NA, Lopes LR, Acatauassu R, et al. Evidence for increased expression of tissue factor and protease-activated receptor-1 in human esophageal cancer. Oncol Rep. 2009; 21:1599–604. [PubMed: 19424642]

[8]. Nitori N, Ino Y, Nakanishi Y, Yamada T, Honda K, Yanagihara K, et al. Prognostic significance of tissue factor in pancreatic ductal adenocarcinoma. Clin Cancer Res. 2005; 11:2531–9. [PubMed: 15814630]

[9]. Patry G, Hovington H, Larue H, Harel F, Fradet Y, Lacombe L. Tissue factor expression correlates with disease-specific survival in patients with node-negative muscle-invasive bladder cancer. Int J Cancer. 2008; 122:1592–7. [PubMed: 18058798]

[10]. Maciel EO, Carvalhal GF, da Silva VD, Batista EL Jr. Garicochea B. Increased tissue factor expression and poor nephroblastoma prognosis. J Urol. 2009; 182:1594–9. [PubMed: 19683742]

[11]. Mueller BM, Reisfeld RA, Edgington TS, Ruf W. Expression of tissue factor by melanoma cells promotes efficient hematogenous metastasis. Proc Natl Acad Sci U S A. 1992; 89:11832–6. [PubMed: 1465406]

[12]. Palumbo JS, Degen JL. Mechanisms linking tumor cell-associated procoagulant function to tumor metastasis. Thromb Res. 2007; 120(Suppl 2):S22–S28. [PubMed: 18023710]

[13]. Sawada M, Miyake S, Ohdama S, Matsubara O, Masuda S, Yakumaru K, et al. Expression of tissue factor in non-small-cell lung cancers and its relationship to metastasis. Br J Cancer. 1999; 79:472–7. [PubMed: 10027315]

[14]. Nakasaki T, Wada H, Shigemori C, Miki C, Gabazza EC, Nobori T, et al. Expression of tissue factor and vascular endothelial growth factor is associated with angiogenesis in colorectal cancer. Am J Hematol. 2002; 69:247–54. [PubMed: 11921018]

[15]. Poon RT, Lau CP, Ho JW, Yu WC, Fan ST, Wong J. Tissue factor expression correlates with tumor angiogenesis and invasiveness in human hepatocellular carcinoma. Clin Cancer Res. 2003; 9:5339–45. [PubMed: 14614019]

[16]. Khorana AA, Ahrendt SA, Ryan CK, Francis CW, Hruban RH, Hu YC, et al. Tissue factor expression, angiogenesis, and thrombosis in pancreatic cancer. Clin Cancer Res. 2007; 13:2870–5. [PubMed: 17504985]

[17]. Zhang Y, Deng Y, Luther T, Muller M, Ziegler R, Waldherr R, et al. Tissue factor controls the balance of angiogenic and antiangiogenic properties of tumor cells in mice. J Clin Invest. 1994; 94:1320–7. [PubMed: 7521887]

[18]. Ruf W, Disse J, Carneiro-Lobo TC, Yokota N, Schaffner F. Tissue factor and cell signalling in cancer progression and thrombosis. J Thromb Haemost. 2011; 9:306–15. [PubMed: 21781267]

[19]. Versteeg HH, Schaffner F, Kerver M, Petersen HH, Ahamed J, Felding-Habermann B, et al. Inhibition of tissue factor signaling suppresses tumor growth. Blood. 2008; 111:190–9. [PubMed: 17901245]

[20]. Markovic SN, Erickson LA, Rao RD, Weenig RH, Pockaj BA, Bardia A, et al. Malignant melanoma in the 21st century, part 1: epidemiology, risk factors, screening, prevention, and diagnosis. Mayo Clin Proc. 2007; 82:364–80. [PubMed: 17352373]

[21]. Markovic SN, Erickson LA, Rao RD, Weenig RH, Pockaj BA, Bardia A, et al. Malignant melanoma in the 21st century, part 2: staging, prognosis, and treatment. Mayo Clin Proc. 2007; 82:490–513. [PubMed: 17418079]

[22]. Ornstein DL, Zacharski LR. Treatment of cancer with anticoagulants: rationale in the treatment of melanoma. Int J Hematol. 2001; 73:157–61. [PubMed: 11372726]

[23]. Amarzguioui M, Peng Q, Wiiger MT, Vasovic V, Babaie E, Holen T, et al. Ex vivo and in vivo delivery of anti-tissue factor short interfering RNA inhibits mouse pulmonary metastasis of B16 melanoma cells. Clin Cancer Res. 2006; 12:4055–61. [PubMed: 16818705]

[24]. Niers TM, Bruggemann LW, Klerk CP, Muller FJ, Buckle T, Reitsma PH, et al. Differential effects of anticoagulants on tumor development of mouse cancer cell lines B16, K1735 and CT26 in lung. Clin Exp Metastasis. 2009; 26:171–8. [PubMed: 19067186]

[25]. Francischetti IM, Valenzuela JG, Andersen JF, Mather TN, Ribeiro JM. Ixolaris, a novel recombinant tissue factor pathway inhibitor (TFPI) from the salivary gland of the tick, Ixodes scapularis: identification of factor X and factor Xa as scaffolds for the inhibition of factor VIIa/tissue factor complex. Blood. 2002; 99:3602–12. [PubMed: 11986214]

[26]. Monteiro RQ, Rezaie AR, Ribeiro JM, Francischetti IM. Ixolaris: a factor Xa heparin-binding exosite inhibitor. Biochem J. 2005; 387:871–7. [PubMed: 15617517]

[27]. Monteiro RQ, Rezaie AR, Bae JS, Calvo E, Andersen JF, Francischetti IM. Ixolaris binding to factor X reveals a precursor state of factor Xa heparin-binding exosite. Protein Sci. 2008; 17:146–53. [PubMed: 18042685]

[28]. Nazareth RA, Tomaz LS, Ortiz-Costa S, Atella GC, Ribeiro JM, Francischetti IM, et al. Antithrombotic properties of Ixolaris, a potent inhibitor of the extrinsic pathway of the coagulation cascade. Thromb Haemost. 2006; 96:7–13. [PubMed: 16807644]

[29]. Andersen JF, Ding XD, Balfour C, Shokhireva TK, Champagne DE, Walker FA, et al. Kinetics and equilibria in ligand binding by nitrophorins 1-4: evidence for stabilization of a nitric oxide-ferriheme complex through a ligand-induced conformational trap. Biochemistry. 2000; 39:10118–31. [PubMed: 10956000]

[30]. Petersen LC, Norby PL, Branner S, Sorensen BB, Elm T, Stennicke HR, et al. Characterization of recombinant murine factor VIIa and recombinant murine tissue factor: a human-murine species compatibility study. Thromb Res. 2005; 116:75–85. [PubMed: 15850611]

[31]. Fernandes RS, Kirszberg C, Rumjanek VM, Monteiro RQ. On the molecular mechanisms for the highly procoagulant pattern of C6 glioma cells. J Thromb Haemost. 2006; 4:1546–52. [PubMed: 16839352]

[32]. Machado DE, Abrao MS, Berardo PT, Takiya CM, Nasciutti LE. Vascular density and distribution of vascular endothelial growth factor (VEGF) and its receptor VEGFR-2 (Flk-1) are significantly higher in patients with deeply infiltrating endometriosis affecting the rectum. Fertil Steril. 2008; 90:148–55. [PubMed: 17765237]

[33]. Knudsen T, Olsen OH, Petersen LC. Tissue factor and factor VIIa cross-species compatibility. Front Biosci. 2011; 17:3196–215. [PubMed: 21622229]

[34]. Zhao J, Aguilar G, Palencia S, Newton E, Abo A. rNAPc2 inhibits colorectal cancer in mice through tissue factor. Clin Cancer Res. 2009; 15:208–16. [PubMed: 19118048]

[35]. Carneiro-Lobo TC, Konig S, Machado DE, Nasciutti LE, Forni MF, Francischetti IM, et al. Ixolaris, a tissue factor inhibitor, blocks primary tumor growth and angiogenesis in a glioblastoma model. J Thromb Haemost. 2009; 7:1855–64. [PubMed: 19624457]

[36]. Mizurini DM, Francischetti IMB, Andersen JF, Monteiro RQ. Nitrophorin 2, a factor IX(a)-directed anticoagulant, inhibits arterial thrombosis without impairing haemostasis. Thromb Haemost. 2010; 104:1116–23. [PubMed: 20838739]

[37]. Isawa H, Yuda M, Yoneda K, Chinzei Y. The insect salivary protein, prolixin-S, inhibits factor IXa generation and Xase complex formation in the blood coagulation pathway. J Biol Chem. 2000; 275:6636–41. [PubMed: 10692472]

[38]. Kirszberg C, Lima LG, Da Silva de OA, Pickering W, Gray E, Barrowcliffe TW, et al. Simultaneous tissue factor expression and phosphatidylserine exposure account for the highly procoagulant pattern of melanoma cell lines. Melanoma Res. 2009; 19:301–8. [PubMed: 19550359]

[39]. Esumi N, Fan D, Fidler IJ. Inhibition of murine melanoma experimental metastasis by recombinant desulfatohirudin, a highly specific thrombin inhibitor. Cancer Res. 1991; 51:4549–56. [PubMed: 1873799]

[40]. Hembrough TA, Swartz GM, Papathanassiu A, Vlasuk GP, Rote WE, Green SJ, et al. Tissue factor/factor VIIa inhibitors block angiogenesis and tumor growth through a nonhemostatic mechanism. Cancer Res. 2003; 63:2997–3000. [PubMed: 12782609]

[41]. Donnelly KM, Bromberg ME, Milstone A, Madison McNiff JM, Terwilliger G, Konigsberg WH, et al. Ancylostoma caninum anticoagulant peptide blocks metastasis in vivo and inhibits factor Xa binding to melanoma cells in vitro. Thromb Haemost. 1998; 79:1041–7. [PubMed: 9609244]

[42]. Palumbo JS, Kombrinck KW, Drew AF, Grimes TS, Kiser JH, Degen JL, et al. Fibrinogen is an important determinant of the metastatic potential of circulating tumor cells. Blood. 2000; 96:3302–9. [PubMed: 11071621]

[43]. Langer F, Amirkhosravi A, Ingersoll SB, Walker JM, Spath B, Eifrig B, et al. Experimental metastasis and primary tumor growth in mice with hemophilia A. J Thromb Haemost. 2006; 4:1056–62. [PubMed: 16689759]

[44]. Palumbo JS, Barney KA, Blevins EA, Shaw MA, Mishra A, Flick MJ, et al. Factor XIII transglutaminase supports hematogenous tumor cell metastasis through a mechanism dependent on natural killer cell function. J Thromb Haemost. 2008; 6:812–9. [PubMed: 18315549]

[45]. Nierodzik ML, Chen K, Takeshita K, Li JJ, Huang YQ, Feng XS, et al. Protease-activated receptor 1 (PAR-1) is required and rate-limiting for thrombin-enhanced experimental pulmonary metastasis. Blood. 1998; 92:3694–700. [PubMed: 9808563]

[46]. Bromberg ME, Bailly MA, Konigsberg WH. Role of protease-activated receptor 1 in tumor metastasis promoted by tissue factor. Thromb Haemost. 2001; 86:1210–4. [PubMed: 11816709]

[47]. Kirszberg C, Rumjanek VM, Monteiro RQ. Assembly and regulation of prothrombinase complex on B16F10 melanoma cells. Thromb Res. 2005; 115:123–9. [PubMed: 15567463]

[48]. Yin YJ, Salah Z, Maoz M, Ram SC, Ochayon S, Neufeld G, et al. Oncogenic transformation induces tumor angiogenesis: a role for PAR1 activation. FASEB J. 2003; 17:163–74. [PubMed: 12554695]

[49]. Villares GJ, Zigler M, Wang H, Melnikova VO, Wu H, Friedman R, et al. Targeting melanoma growth and metastasis with systemic delivery of liposome-incorporated protease-activated receptor-1 small interfering RNA. Cancer Res. 2008; 68:9078–86. [PubMed: 18974154]

[50]. Yang E, Boire A, Agarwal A, Nguyen N, O'Callaghan K, Tu P, et al. Blockade of PAR1 signaling with cell-penetrating pepducins inhibits Akt survival pathways in breast cancer cells

and suppresses tumor survival and metastasis. Cancer Res. 2009; 69:6223–31. [PubMed: 19622769]

[51]. Hu L, Lee M, Campbell W, Perez-Soler R, Karpatkin S. Role of endogenous thrombin in tumor implantation, seeding, and spontaneous metastasis. Blood. 2004; 104:2746–51. [PubMed: 15265791]

[52]. Versteeg HH, Schaffner F, Kerver M, Ellies LG, Andrade-Gordon P, Mueller BM, et al. Protease-activated receptor (PAR) 2, but not PAR1, signaling promotes the development of mammary adenocarcinoma in polyoma middle T mice. Cancer Res. 2008; 68:7219–27. [PubMed: 18757438]

[53]. Dutra-Oliveira A, Monteiro RQ, Mariano-Oliveira A. Protease-activated receptor-2 (PAR2) mediates VEGF production through the ERK1/2 pathway in human glioblastoma cell lines. Biochem Biophys Res Commun. 2012; 421:221–7. [PubMed: 22497886]

[54]. Depasquale I, Thompson WD. Prognosis in human melanoma: PAR-1 expression is superior to other coagulation components and VEGF. Histopathology. 2008; 52:500–9. [PubMed: 18315603]

[55]. Cocco E, Varughese J, Buza N, Bellone S, Glasgow M, Bellone M, et al. Expression of tissue factor in adenocarcinoma and squamous cell carcinoma of the uterine cervix: implications for immunotherapy with hI-con1, a factor VII-IgGFc chimeric protein targeting tissue factor. BMC Cancer. 2011; 11:263. [PubMed: 21693061]

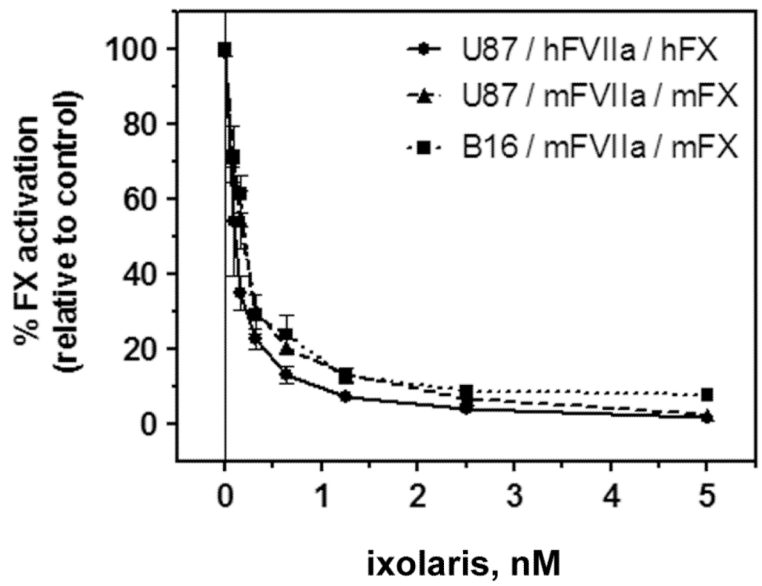

Figure 1. Ixolaris blocks murine and human TF procoagulant activity to a similar extent

The inhibitory effect of ixolaris on the TF activity of U87-MG human glioblastoma and B16F10 murine melanoma cell lines was tested by examining activation of FX by FVIIa in the presence of the cells. U87-MG and B16F10 cells were incubated with FVIIa [murine (mFVIIa) or human (hFVIIa) origin] for 10 min prior to the addition of FX [murine (mFX) or human (hFX) origin], either pre-incubated or not with varying amounts of ixolaris (0-5 nM). The amount of FXa formed was measured after 30 min of reaction time. Results are expressed as the percentage of FXa activation relative to the control sample not incubated with ixolaris (0 nM). Each data point represents the mean ± SD of replicates from three independent experiments. The assay conditions are described in the Methods section.

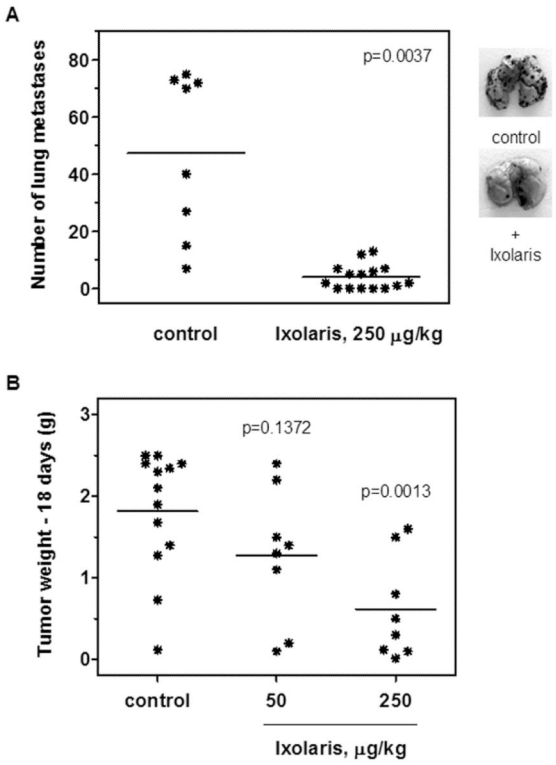

Figure 2. Ixolaris inhibits the establishment of B16F10 melanoma cells *in vivo*

(A) B16F10 cells (2.5×10^5) were injected intravenously into C57BL/6 mice after previous injection of ixolaris (250 μg/kg) or PBS (see Materials and Methods). After 15 days, tumor nodules on harvested lungs were counted. Lines represent the mean of the number of pulmonary tumor nodules observed in the animals from each group. Representative lungs of each group are shown. (B) B16F10 cells (3.5×10^5) were injected subcutaneously into C57BL/6 mice. Daily treatment with ixolaris was initiated 3 days after tumor cell inoculation. Control animals were treated with an equivalent volume of PBS. After 18 days of tumor cell inoculation, the animals were sacrificed and the tumors were removed and weighed. Lines represent the mean of tumor weight in each group.

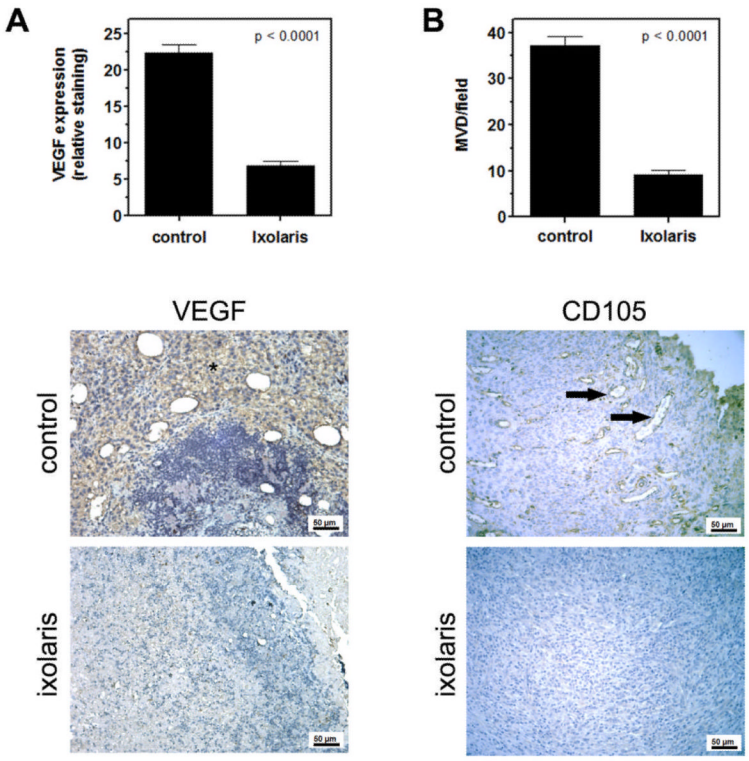

Figure 3. Ixolaris treatment reduces angiogenesis in primary melanoma tumors

(A) Quantification of VEGF staining in tumor masses was performed as described in the Methods section. Bars show the decrease of relative VEGF staining in the primary tumors of animals treated with ixolaris (n=5; 6.8 ± 3.3) as compared to the control group (n=5; 22.4 ± 5.4). Representative images of VEGF staining (asterisk) are shown below. (B) Vessel density was evaluated in CD105-stained sections of the primary tumors, as described in the Methods section. Bars show the decrease of CD105 expression in the primary tumors of animals treated with ixolaris (n=5; 9.1 ± 3.5) as compared to the control group (n=5; 37.2 ± 6.1). Representative images of CD105 staining (arrows) are shown below. Values are given as the mean ± SD of each group.

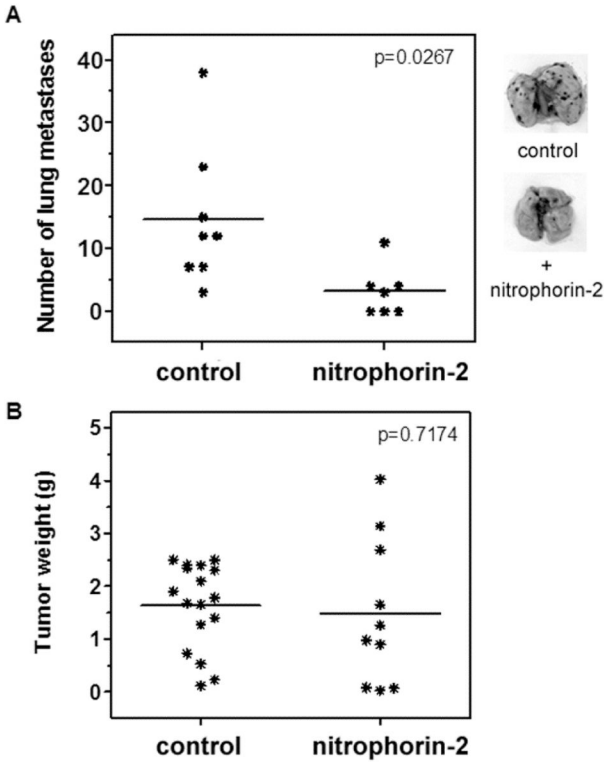

Figure 4. Nitrophorin-2 reduces metastasis of B16F10 cells but has no effect on the primary tumor growth *in vivo*

(A) B16F10 cells (2.5×10^5) were injected intravenously into C57BL/6 mice after previous injection of nitrophorin-2 (250 μg/kg) or PBS (see Materials and Methods). After 15 days, the tumor nodules on harvested lungs were counted. Lines represent the mean of the number of pulmonary tumor nodules observed in the animals from each group. Representative lungs of each group are shown. (B) B16F10 cells (3.5×10^5) were injected subcutaneously into C57BL/6 mice. Daily treatment with nitrophorin-2 (250 μg/kg) was initiated 3 days after tumor cell inoculation. The control animals were treated with an equivalent volume of PBS. After 18 days of tumor cell inoculation, the animals were sacrificed, and the tumors were removed and weighed. Lines represent the mean of tumor weight in each group.

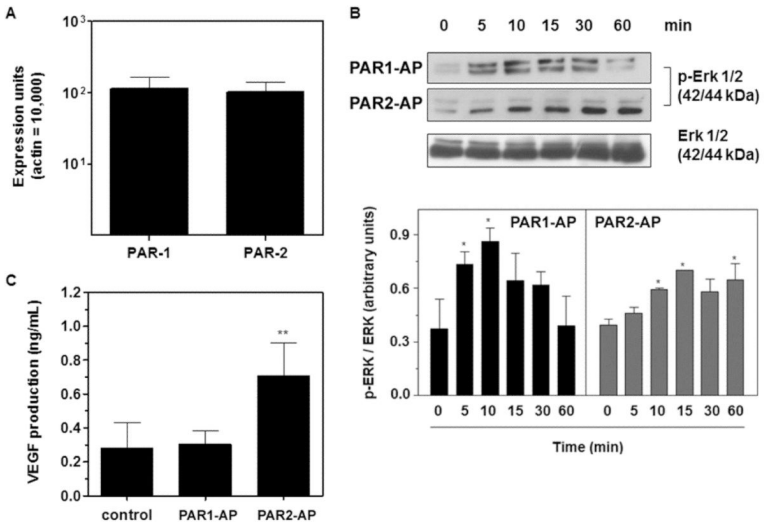

Figure 5. PAR2 but not PAR1 mediates VEGF production by B16F10 cells *in vitro*

(A) Real-time PCR analysis of PAR1 and PAR2 gene expression in B16F10 cells. The assay was performed as described in the Methods section. Bars represent the mean ± SD of three independent experiments. (B) PAR1 and PAR2 mediate ERK 1/2 activation in B16F10 cells. B16F10 cells were serum-starved for 30 min and then treated with PAR1 (PAR1-AP, TFLLR-NH2, 50 μM) or PAR2 (PAR2-AP, SLIGKL-NH2, 50 μM) agonist peptides for different lengths of time. The levels of total and phosphorylated ERK 1/2 in the cell lysates were determined by immunoblotting, as described in the Methods section, and quantified by densitometry using the Scion Image software. Bars represent the mean ± SD of three independent experiments. Asterisks (*) indicate $p<0.05$ relative to time=0 min. (C) VEGF production by B16F10 cells mediated by PAR1 or PAR2 activation. The concentrations of VEGF in the supernatants of B16F10 cells cultured in the absence (control) or in the presence of PAR1 (PAR1-AP, TFLLR-NH2, 50 μM) or PAR2 (PAR2-AP, SLIGKL-NH2, 50 μM) agonist peptides for 24 h were assessed by ELISA. Bars represent the mean ± SD of three independent experiments. Asterisks (**) indicate $p<0.01$ relative to control.

Table 1
Primer sequences employed in Real-time PCR assays

Genes	Amplicon size (bases)	Primer Sequence (5′–3′)
PAR1	124	GCA GGC CAG AAT CAA AAG CAA CAT TTT TCT CCT CAT CCT CCC
PAR2	129	AAG GTT GAT GGC ACA TCC CAC AGT GGT CAG TTT TCC AGT GAG
β-actin	122	ATG GTG GGA ATG GGT CAG AAG TTC TCC ATG TCG TCC CAG TTG